International Journal of Electrical and Computer Engineering (IJECE)
Vol. 15, No. 5, October 2025, pp. 4409~4420
ISSN: 2088-8708, DOI: 10.11591/ijece.v15i5.pp4409-4420

Optimized fractional-order direct torque control with space vector modulation strategy for two-wheel-drive electric vehicles

Touhami Nawal[1], Ouled-Ali Omar[1], Mansouri Smail[2], Benhammou Aissa[3]
[1]LDDI Laboratory, Department of Electrical Engineering, Faculty of Technology, Ahmed Draia University, Adrar, Algeria
[2]LEESI Laboratory, Department of Electrical Engineering, Faculty of Technology, Ahmed Draia University, Adrar, Algeria
[3]SGRE Laboratory, Department of Electrical Engineering, Faculty of Technology, Mohamed Tahri University, Bechar, Algeria

Article Info

Article history:

Received Dec 12, 2024
Revised May 29, 2025
Accepted Jul 3, 2025

Keywords:

Direct torque control with space vector modulation
Electronic differential
Fractional order PID
Grey wolf optimization
Permanent magnet synchronous motor
Two-wheel drive electric vehicle

ABSTRACT

Electric vehicles (EVs) are a sustainable and efficient transportation choice, offering zero emissions, lower operating costs, and advanced performance features like instant torque and regenerative braking. They promote energy independence, improve urban livability, and support the global shift toward cleaner, renewable energy-powered mobility, making them a future-proof investment. The electric motor is a critical component in electric vehicles (EVs), the importance of which lies in its high efficiency, instant torque delivery, and smooth operation, which enhances performance and energy use. This paper focuses on a two-wheel drive electric vehicle (TWD EV) configuration powered by an energy storage battery system (ESBS), driven by two permanent magnet synchronous motors (PMSMs), and controlled using direct torque control with space vector modulation (DTC-SVM). fractional-order proportional integral derivative (FOPID) controllers, optimized via the grey wolf optimizer (GWO) algorithm, are implemented for precise speed control of the PMSMs. An electronic differential (ED) is incorporated to ensure vehicle stability, safety, and performance. The simulation results show that the proposed GWO-FOPID controller gave super results by reducing electromagnetic torque overshoot by 33%, improves torque settling time by 55%, and achieves the lowest electromagnetic torque ripple of approximately ±1 Nm compared to conventional DTC-SVM and GWO-PID approaches. Additionally, it optimized speed overshoot and undershoot by 44%, significantly enhancing system performance, responsiveness, and drive smoothness. This novel combination of fractional-order control, metaheuristic optimization, and electronic differential integration marks a meaningful advancement in high-precision and efficient control for 2WD EVs.

Corresponding Author:

Touhami Nawal
LDDI Laboratory, Department of Electrical Engineering, Faculty of Technology, Ahmed Draia University
Adrar, Algeria
Email: touhami.nawal@univ-adrar.edu.dz

1. INTRODUCTION

The transportation sector refers to a major contributor to environmental pollution, a leading cause of climate change [1]. With 24% of these emissions originating from transportation, 72% of which comes from ground transport and continues to rise, there is a pressing need for greater stakeholder involvement in transitioning to green transportation [2]–[4]. Electric vehicles (EVs) are pivotal in reducing emissions and promoting environmental sustainability [5], [6]. As zero-emission vehicles, EVs address the environmental challenges posed through fossil fuel powered vehicles and are widely regarded as the future of transportation

for their ability to curb rising fuel costs and air pollution [6], [7]. Electric motors are integral to the powertrain of EVs, playing a crucial role in their functionality [8]. Several studies have explored optimal motor technologies for EV applications. Rimpas *et al.* [9] conducted a comprehensive review of various motor technologies, including synchronous motors, induction motors and brushless motors, commonly employed in electric vehicles. The study determined that both induction motors and permanent magnet motors emerge as ideal choices when evaluated against all relevant criteria.

In terms of motor control strategies, direct torque control (DTC) has gained attention for its simplicity and dynamic performance. Bobin and Beno [10] highlighted that DTC offers several advantages over field-oriented control (FOC). DTC demonstrates greater resistance to external disturbances, adapts better to variations in operating conditions, and eliminates the need for reference frame transformations [11]. Additionally, it provides a superior dynamic response compared to the FOC method. Furthermore, Mesloub *et al.* [12] conducted a study involving both simulation and real-world implementation of traditional DTC and DTC-SVM for PMSMs. The findings indicate that the SVM-based approach delivers superior performance in comparison to traditional DTC, notably in reducing flux and torque ripples.

In addition to selecting an effective control strategy, the design of the controller itself is critical. Agarwal *et al.* [13] demonstrated that fractional-order controllers offer greater flexibility in adjusting the time and frequency responses of control systems compared to traditional PID controllers, making fractional-order proportional-integral-derivative (FOPID) a more effective option. Ahmed *et al.* [14] further enhanced FOPID performance by using a hybrid grey wolf optimizer (GWO), demonstrating that the GWO-FOPID approach significantly improved the drive system's dynamic response and control accuracy over conventional PID methods. To enhance vehicle stability and safety, Hartani *et al.* [15] demonstrated that the electronic differential precisely regulates the speeds of the driving wheels, ensuring high accuracy on both flat and curved roads.

Expanding on previous research, this study presents an innovative control strategy for two-wheel-drive electric vehicles (TWD EV), incorporating FOPID controllers optimized through the recent GWO, integrated in DTC-SVM technique for robust and efficient motor management, and an electronic differential (ED) for precise wheel speed coordination and vehicle stability. The proposed system brings several novel contributions: adaptive tuning of FOPID controllers via the GWO metaheuristic algorithm to enhance control responsiveness and parameter optimization; integration of DTC-SVM with GWO-FOPID to deliver accurate torque and speed regulation while minimizing computational burden; and the use of an electronic differential to improve handling and traction, particularly during cornering. Collectively, these innovations represent a significant advancement in developing smart, high-performance, and dependable control solutions for modern electric vehicle applications.

This article is structured into 8 sections where section 2 displays the PMSM model, section 3 explains the DTC-SVM control technique of the proposed motors, section 4 illustrates the FOPID controllers, the section 5 explains the metaheuristic algorithm, section 6 illustrate the TWD EV model, section 7 covers the simulation and results, and the conclusions of this contribution are provided in the last section.

2. PMSM MATHEMATICAL MODEL

To illustrate the use of variable speed control, the modeling of the permanent magnet synchronous machine (PMSM) is based on standard mechanical and electrical parameters. These parameters describe the machine's electromechanical and electromagnetic behavior. The model also includes a set of simplifying assumptions to facilitate analysis and simulation as follow: iron saturation in the motor's stator is ignored, hysteresis effects and eddy current are disregarded, and the three-phase windings of the stator are assumed to be symmetrical [16]. The mathematical model of thePMSM in the α-β coordinate system is as follows [17]:

$$\text{Voltage equations: } \begin{cases} U_\alpha = R_s I_\alpha + \frac{d\Phi_\alpha}{dt} \\ U_\beta = R_s I_\beta + \frac{d\Phi_\beta}{dt} \end{cases} \quad (1)$$

Equations (1) describe the voltages across the stator windings, incorporating the resistive component and the time-varying magnetic flux. They represent the dynamic behavior of the stator in the α-β reference frame.

$$\text{Magnetic chain equations : } \begin{cases} \Phi_\alpha = L_s I_\alpha + \Phi_f \\ \Phi_\beta = L_s I_\beta + \Phi_f \end{cases} \quad (2)$$

These expressions define the magnetic flux linkage for each axis, combining the stator's self-inductance and the constant flux from the rotor magnets. The model assumes that the stator has identical inductance values along both the α and β axes due to symmetry.

$$\text{Back electromotive force equations : } \begin{cases} e_\alpha = \frac{d\Phi_f cos\theta_e}{dt} = -\omega_e \Phi_f sin\theta_e \\ e_\beta = \frac{d\Phi_f cos\theta_e}{dt} = -\omega_e \Phi_f sin\theta_e \end{cases} \quad (3)$$

These equations quantify the back EMF generated in the stator windings as a result of rotor rotation. They are essential for estimating rotor speed and position.

The equation for electromagnetic torque and the motion equation of the PMSM in the d-q plan of the rotating reference frame.

$$\begin{cases} T_e = \frac{3N_p \Phi_f I_q}{2} \\ J\frac{d\omega_m}{dt} = T_e - T_L - B\omega_m \end{cases} \quad (4)$$

The electromagnetic torque T_e is directly related to the q-axis current I_q and the permanent magnet flux Φ_f. The second equation models the rotor's rotational dynamics, where the change in angular speed depends on the net torque after subtracting load torque and mechanical friction. This is essentially a rotational form of Newton's second law.

Where U_α, U_β represent the voltage components in the α-β plan; I_α, I_β denote the values of the current along the α-β plan; Φ_α, Φ_β refer to the values of the magnetic flux along the α-β plan; R_s is the stator resistor; L_s is inductance of the stator; Φ_f represents the permanent magnet flux linkage; e_α, e_β are the induced electromotive forces along the α-β plane; ω_e is the rotor's electrical angular velocity; N_p is the number of poles; I_q is the current along the q-axis; ω_m is the rotational angular velocity; J is the moment of inertia; B is the damping coefficient; T_e is the motor's electromagnetic torque; T_L is the motor's load torque.

3. DIRECT TORQUE CONTROL WITH SPACE VECTOR MODULATION CONTROL OF PMSM

The direct torque control with space vector modulation (DTC-SVM) strategy enhances traditional DTC by significantly minimizing torque ripple, a common issue caused by the inaccurate positioning of the stator flux vector. In this improved approach, the control system still receives the torque and stator flux commands as inputs, but instead of using hysteresis controllers and switching tables, it incorporates proportional-integral (PI) controllers for both torque and flux regulation. The PI controller for torque generates a load angle command (δ*) based on the torque error, while the flux controller produces a voltage angle command to ensure precise positioning of the stator flux according to the motor's real-time rotational speed and estimated flux linkage. These two outputs—the load angle and voltage angle commands—are used to synthesize a reference stator voltage vector, which is then applied to the inverter through a space vector modulation (SVM) block. This modulation technique allows for smooth and continuous switching at a constant frequency, improving overall motor performance, reducing torque and flux ripples, and increasing the efficiency and stability of the drive system [18]. Figure 1 presents the implementation of this DTC-SVM control model for the permanent magnet synchronous motor (PMSM) using MATLAB/Simulink.

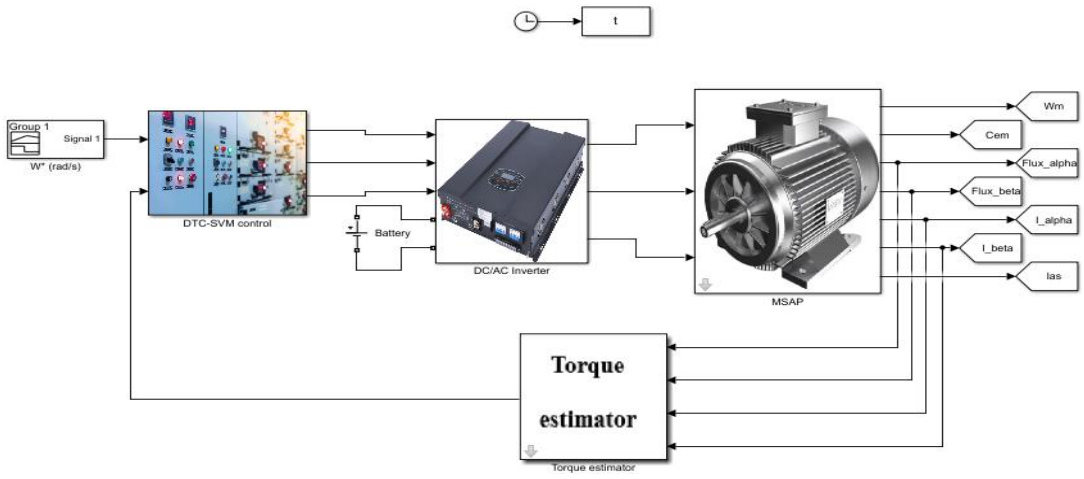

Figure 1. Simulink block of DTC-SVM control for PMSM used in this study

4. FRACTIONAL-ORDER PROPORTIONAL INTEGRAL DERIVATIVE CONTROLLER

Before designing a fractional-order proportional-integral-derivative (FOPID) controller, it is essential to understand the fundamental concepts of fractional-order (FO) calculus, particularly the FO-derivative and FO-integral operators. These operators extend the concept of differentiation and integration to non-integer (fractional) orders, providing more flexible and precise dynamic modeling tools. The mathematical foundations and properties of FO operators are well documented in the literature and have led to a growing interest in applying fractional calculus in control systems. The FOPID controller, first introduced in 1999, extends the classical PID controller by incorporating two additional parameters λ and μ representing the orders of integration and differentiation, respectively. The general mathematical expression of the FOPID controller is [19]:

$$C(s) = K_p + \frac{K_i}{S^{\lambda}} + K_d S^{\mu} \tag{5}$$

where λ and μ can vary between 0 and 2 [20], k_p, k_i, and k_d represent the controller's positive gains. Unlike the traditional PID controller [21], which is limited to integer-order operations, the FOPID controller's tunable λ and μ parameters offer greater flexibility in shaping system dynamics. This allows for more effective tuning and improved performance across a broader range of system conditions, making FOPID controllers particularly advantageous in complex or highly nonlinear systems [22], [23].

5. METAHEURISTIC ALGORITHM GREY WOLF OPTIMIZER

In 2014, Seyedali Mirjalili and colleagues introduced the grey wolf optimizer (GWO), an innovative metaheuristic algorithm inspired by the natural hunting tactics and social dynamics of grey wolf packs [24]. This algorithm is grounded in the observation that grey wolves exhibit highly organized and cooperative behaviors during hunting, which enable them to efficiently locate, encircle, and capture prey. In the wild, grey wolves live in structured packs governed by a strict social hierarchy, where each member has a defined role that contributes to the collective success of the group. The GWO models this hierarchy by dividing the population into four distinct levels: alpha (α), beta (β), delta (δ), and omega (ω). The alpha wolves are the leaders and primary decision-makers who determine the pack's hunting strategy and direct movements. Betas serve as advisors and are second-in-command, helping to refine strategies and potentially taking over leadership if needed. Deltas act as subordinates who assist with hunting and scouting tasks, supporting the alphas and betas. Finally, the omegas occupy the lowest rank, maintaining pack cohesion and following the lead of higher-ranked wolves. The hunting behavior itself is characterized by three main phases: tracking the prey, chasing it, and finally attacking, which the algorithm mathematically emulates. In the GWO's mathematical model, it is assumed that the top three wolves α, β, and δ have an accurate understanding of the prey's position, guiding the search process. The omega wolves then update their positions based on the movements and insights of these leaders, thereby simulating cooperative hunting. This hierarchical and social hunting approach allows the GWO to balance exploration and exploitation effectively in complex optimization problems, making it a versatile and powerful algorithm for solving a wide range of engineering and computational challenges [25], [26]. The corresponding mathematical formulas are provided below [26]:

$$\begin{cases} \overrightarrow{D_\alpha} = \left|\overrightarrow{C_1}.\overrightarrow{X_\alpha} - \overrightarrow{X_i}(t)\right| \\ \overrightarrow{D_\beta} = \left|\overrightarrow{C_2}.\overrightarrow{X_\beta} - \overrightarrow{X_i}(t)\right| \\ \overrightarrow{D_\delta} = \left|\overrightarrow{C_3}.\overrightarrow{X_\delta} - \overrightarrow{X_i}(t)\right| \end{cases} \tag{6}$$

$$\begin{cases} \overrightarrow{X_1} = \left|\overrightarrow{X_\alpha} - \overrightarrow{A_1}.\overrightarrow{D_\alpha}\right| \\ \overrightarrow{X_2} = \left|\overrightarrow{X_\beta} - \overrightarrow{A_2}.\overrightarrow{D_\beta}\right| \\ \overrightarrow{X_3} = \left|\overrightarrow{X_\delta} - \overrightarrow{A_3}.\overrightarrow{D_\delta}\right| \end{cases} \tag{7}$$

$$\overrightarrow{X_i}(t+1) = \frac{\overrightarrow{X_1}+\overrightarrow{X_2}+\overrightarrow{X_3}}{3} \tag{8}$$

$$\vec{A} = 2.\vec{a}.\overrightarrow{r_1} - \vec{a} \tag{9}$$

$$\vec{C} = 2.\overrightarrow{r_2} \tag{10}$$

$$\vec{a} = 2.\left(1 - \frac{t}{T_{max}}\right) \quad (11)$$

Where:
$\overrightarrow{X_\alpha}, \overrightarrow{X_\beta}, \overrightarrow{X_\delta}$ denote the position vectors corresponding to the alpha, beta, and delta wolves, respectively.
$\overrightarrow{D_\alpha}, \overrightarrow{D_\beta}, \overrightarrow{D_\delta}$ represent refer to the present and subsequent iteration solutions, respectively.
$\vec{A}$, $\vec{C}$ denote the coefficient vectors.
$\overrightarrow{r_1}, \overrightarrow{r_2}$ are random vectors within the range [0, 1].
T_{max} represents the maximum number of iterations.

Figure 2 presents the GWO algorithm's flowchart, illustrating each stage of the process. In PMSM control systems, the GWO is applied to fine-tune parameters such as PID controller gains, aiming to reduce speed error and torque ripple. It identifies optimal values by assessing different parameter combinations through simulations. Key settings like population size and the number of iterations are carefully chosen based on system limitations. Once optimized, these parameters are implemented in real-time control. Overall, GWO enhances control performance and demonstrates the effectiveness of bio-inspired optimization techniques in electric motor applications. Table 1 provides the parameters used for simulating the GWO algorithm.

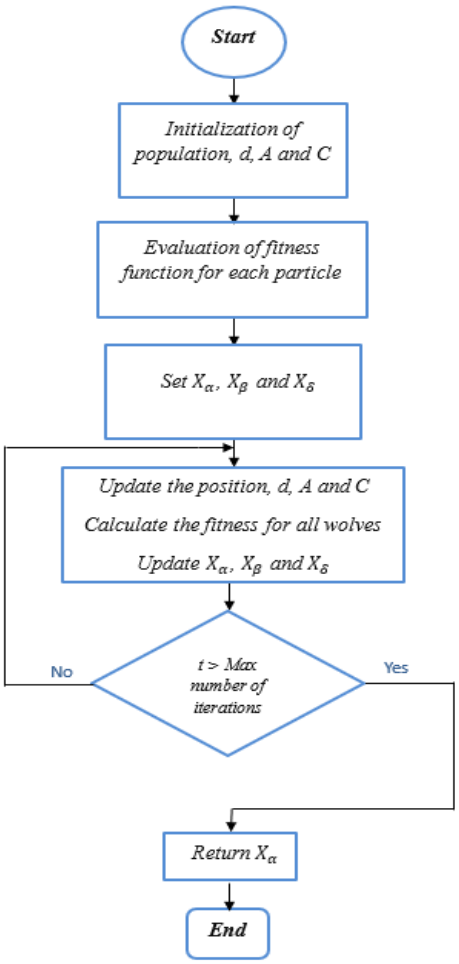

Figure 2. Diagram of the GWO algorithm process [27]

Table 1. The parameters employed in the GWO algorithm

Parameters	Value
Number of search agents	50
Lower bound	0
Upper bound	100
Number of iterations	100

6. TWO-WHEEL DRIVE ELECTRIC VEHICLE SYSTEM

The EV drive system is composed of three fundamental subsystems that work in harmony to ensure efficient and reliable vehicle operation: the energy source, the traction system, and the supplementary subsystem. The energy source subsystem primarily includes the battery, which stores electrical energy, and the DC/DC converter, which manages voltage levels to meet the requirements of various components within the vehicle. The traction subsystem is responsible for converting electrical energy into mechanical motion and includes key components such as the electric motor, power inverters that control the motor's operation, torque transmission mechanisms that deliver power to the wheels, the wheels themselves, and control units that regulate system performance. Complementing these is the supplementary subsystem, which enhances vehicle control and stability; this includes the steering unit [28] and the electronic differential (ED).

Unlike traditional mechanical differentials, which rely on gears to distribute torque and allow wheels to rotate at different speeds, the ED uses electronic control to achieve the same function with greater precision and responsiveness. During cornering, the inner and outer wheels follow different radius, necessitating varying rotational speeds to prevent tire slip and maintain vehicle stability. The ED uses input from the steering wheel control signals to dynamically adjust the speed of each driving wheel, ensuring that the vehicle remains stable and responsive to driver commands. This electronic control also enables advanced stability features such as torque vectoring and enhanced traction control. The behavior and dynamics of the ED are mathematically described by differential equations, which capture the relationship between steering inputs and wheel speeds, enabling accurate simulation and control of the EV's handling characteristics [29].

The differential electronic equation is given in (12) [27]:

$$\begin{cases} W_r^* = C_{red} * W_{ref} * (1 - \frac{d_\omega * tan(\delta)}{2L}) \\ W_l^* = C_{red} * W_{ref} * (1 + \frac{d_\omega * tan(\delta)}{2L}) \end{cases} \quad (12)$$

Where
C_{red} The gear coefficient.
L The wheelbase of the EV.
δ The steering angle.
d_ω The spacing between the wheels on the same axle.
W_r^* and W_l^* The angular velocity of the right and left wheel drives, respectively.
Figure 3 illustrates the primary structure of the 2WD EV proposed in this study, which is governed by an optimized DTC-SVM control system.

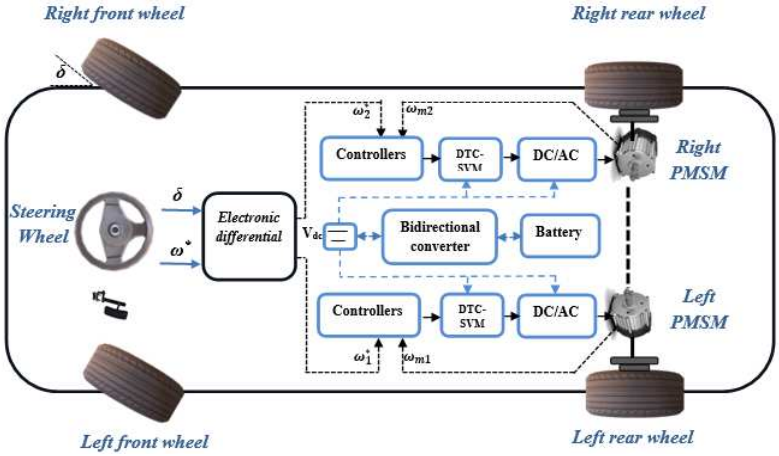

Figure 3. Proposed TWD EV

7. RESULTS AND DISCUSSIONS

In this study, we simulated a TWD EV controlled by DTC-SVM through an electronic differential (ED) with PID controllers then FOPID controllers, optimized using the GWO in MATLAB/Simulink. The ITAE objective function was used to minimize the error over time in the control system. The electric vehicle (EV) was evaluated at different variable speeds, including executing 70 degrees right turn within 0.6 seconds,

40 degrees right turn over 8 seconds, 60 degrees left turn over 15.8 seconds and 60 degrees right turn over 24.8 seconds. Additionally, various resistive torque values were applied, as illustrated in Figure 4.

Figure 5 highlights the wheel speed responses (WD1 and WD2) using DTC-SVM, GWO-PID, and GWO-FOPID controllers. While all controllers accurately track the reference signals, GWO-FOPID stands out with its superior dynamic performance, particularly during rapid transitions such as acceleration, deceleration, and turning. The zoomed subplots (a–d) further confirm that GWO-FOPID consistently offers the fastest, most stable responses with minimal overshoot, especially in asymmetric and high-speed conditions. This demonstrates its enhanced robustness and adaptability in dynamic driving scenarios.

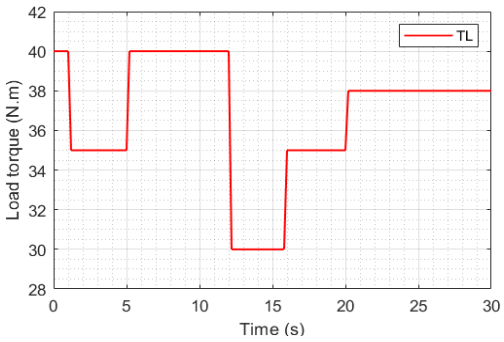

Figure 4. The load torque (T_L) used in our study

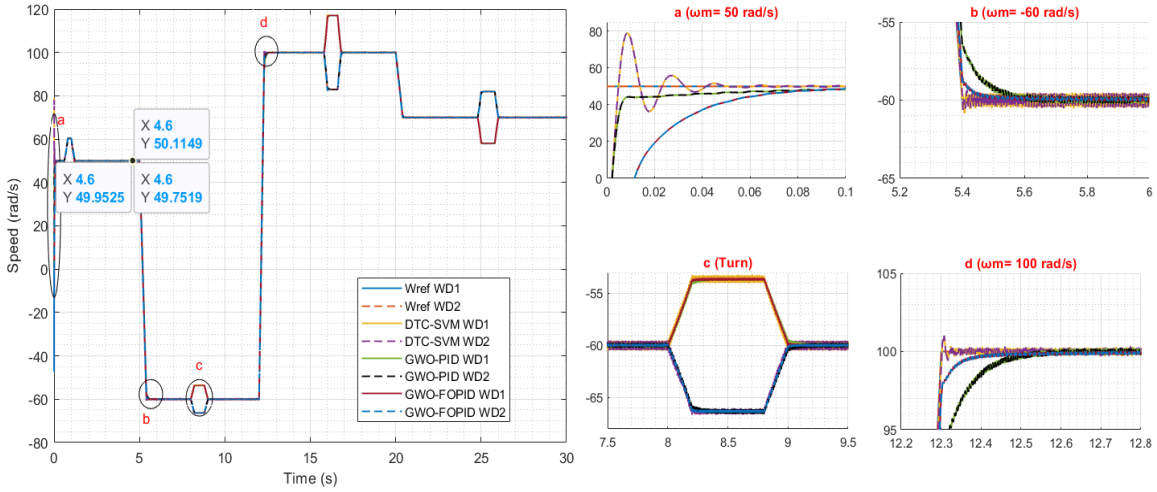

Figure 5. Speed control performances

Figure 6 illustrates the torque response and ripple behavior of different control strategies under varying load conditions. While all controllers follow the torque commands, DTC-SVM shows significant overshoot and oscillations, especially during transitions. GWO-PID improves stability but still exhibits some fluctuations. GWO-FOPID stands out by delivering the most stable and smooth torque response, reducing dynamic disturbances. The detailed subplots further reveal torque ripple patterns during both transient and steady states. DTC-SVM produces the highest ripple, while GWO-PID shows moderate improvement. GWO-FOPID again demonstrates superior performance with minimal ripples, leading to better motor efficiency, less mechanical stress, and enhanced driving comfort.

Figure 7 shows that the current of the right motor increases proportionally with the load torque. This indicates that the control system responds effectively to torque demands, adjusting the current accordingly. The waveform remains stable with minimal distortion, demonstrating good current regulation and confirming the robustness of the proposed control strategy under varying load conditions. Figure 8 illustrates the β-axis versus α-axis flux trajectory of the PMSM. GWO-FOPID achieves a more consistent and tighter elliptical path than DTC-SVM and GWO-PID, indicating better flux control and reduced ripple. This enhanced performance contributes to improved motor efficiency and stability.

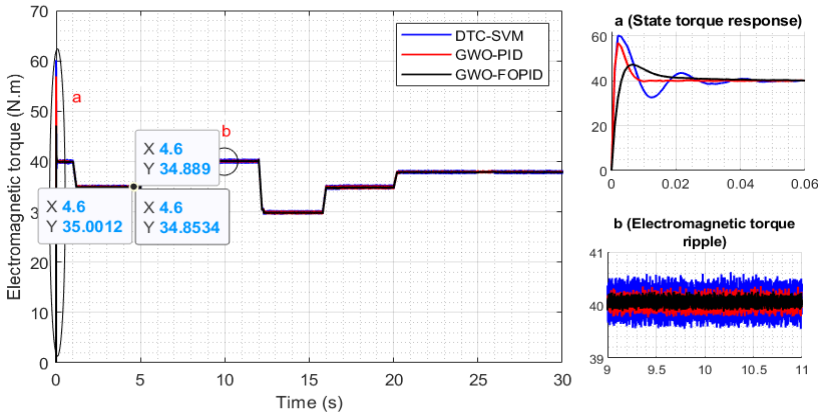

Figure 6. Electromagnetic torque

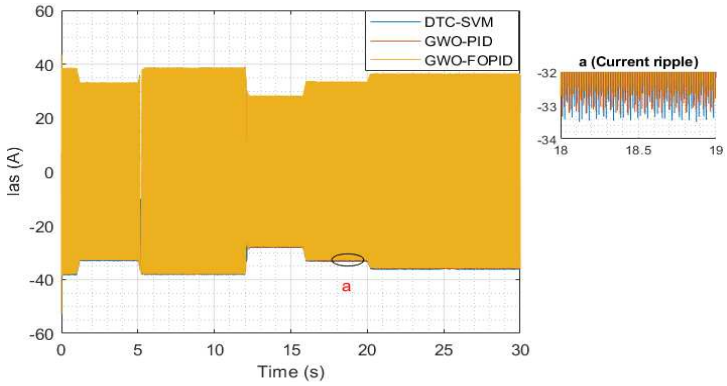

Figure 7. Current of PMSM

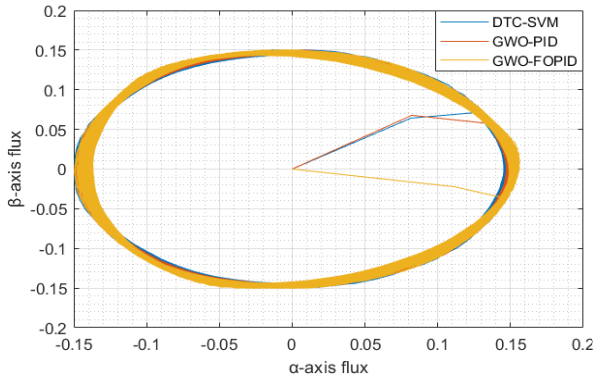

Figure 8. β-axis flux depending on the α-axis flux of PMSM

For speed as shown in Figure 9, the performance comparison highlights that DTC-SVM offers the fastest response time (0.074 s) but at the cost of significant overshot (58.56%) and higher ripple (0.45%). In contrast, GWO-PID and GWO-FOPID exhibit no overshoot, ensuring excellent stability, with GWO-FOPID achieving the lowest ripple (0.15%) and a moderate response time (0.16 s), while GWO-PID shows slightly higher ripple (0.21%) and slower response time (0.23 s). This makes GWO-FOPID the most balanced approach for precision and stability followed by GWO-PID technique.

Regarding electromagnetic torque presented in Figure 10, the comparison shows that DTC-SVM provides a fast response time (0.05 s) but suffers from a high overshoot (50.83%) and ripple (1.4%). GWO-PID achieves the quickest response (0.01 s) with a slightly reduced overshoot (42.3%) and lower ripple

(0.8%). GWO-FOPID balances performance with a moderate response time (0.05 s), significantly reduced overshoot (17.8%), and the lowest ripple (0.5%), making it the most stable and precise option overall.

Based on Figures 5 and 6, at t = 4.6 s, the comparison of the three control methods FOPID-GWO, PID-GWO and DTC-SVM, reveals that the respective angular speeds are 50.1149 rad/s, 49.9507 rad/s, and 49.7519 rad/s, while the corresponding electromagnetic torques are 35.0012 Nm, 34.889 Nm, and 34.8534 Nm. The resulting power outputs are 1754.08 W, 1742.72 W, and 1734.02 W, where the nominal power is 15 kW. These findings demonstrate that the proposed FOPID-GWO strategy consistently delivers superior performance compared to the other methods, establishing it as the most effective control solution among the three.

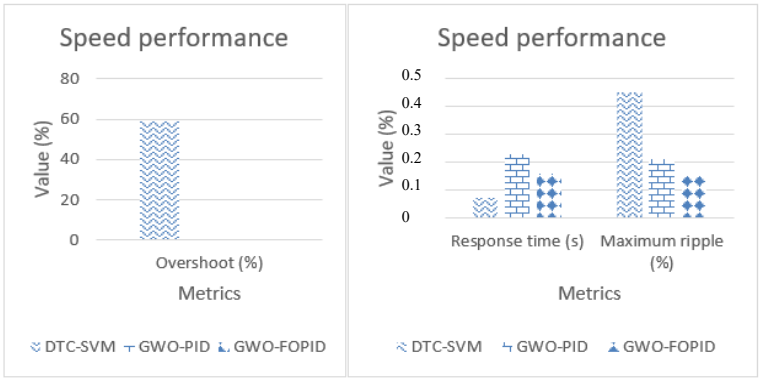

Figure 9. Chart of speed performance of various techniques

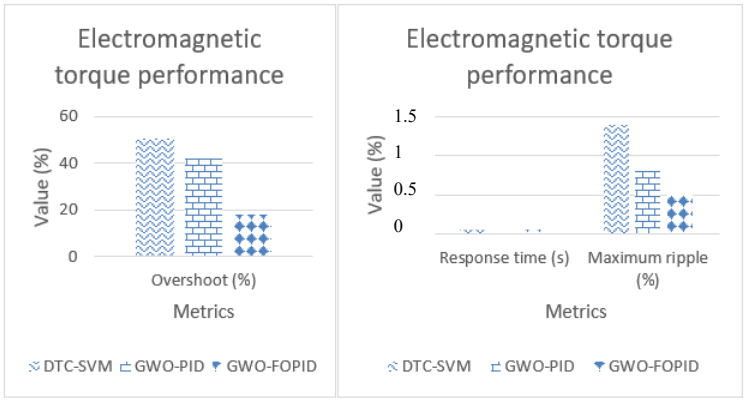

Figure 10. Chart of electromagnetic torque performance of various techniques

8. CONCLUSION

This paper examined a TWD-EV controlled by DTC-SVM, optimized by GWO-PID then GWO-FOPID. The simulation results validate the effectiveness of the proposed GWO-FOPID controller in enhancing the performance of the TWD-EV. Compared to conventional DTC-SVM and GWO-PID methods, the GWO-FOPID approach achieved a 33% reduction in electromagnetic torque overshoot, a 55% improvement in torque settling time, and minimized the electromagnetic torque ripple to approximately ±1 Nm. Furthermore, it optimized speed overshoot and undershoot by 44%, ensuring smoother and more stable vehicle operation. These findings demonstrate the GWO-FOPID controller's superior ability to deliver high-precision, efficient, and robust dynamic performance. The current results are simulation-based, and need to compare to another robust controllers as high-order SMC and MPC to validate the robustness of the proposed techniques, in addition to experimental validation is planned to confirm robustness under real-world conditions. The authors also suggest extending the traction system to four-wheel drives and enhancing the results by integrating multi-objective optimization algorithms, simpler speed estimators, and experimental system validation.

ACKNOWLEDGEMENTS

The authors extend their thanks to the General Direction of Scientific Research and Technological Development, DGRSDT, and the research laboratories of Adrar University and Bechar University including LDDI, LEESI and SGRE.

FUNDING INFORMATION

According to the authors, this work was not supported by any funding source.

AUTHOR CONTRIBUTIONS STATEMENT

This journal uses the Contributor Roles Taxonomy (CRediT) to recognize individual author contributions, reduce authorship disputes, and facilitate collaboration.

Name of Author	C	M	So	Va	Fo	I	R	D	O	E	Vi	Su	P	Fu
Touhami Nawal	✓	✓	✓	✓	✓	✓		✓	✓	✓			✓	
Ouled-Ali Omar		✓			✓	✓		✓	✓	✓	✓	✓		✓
Mansouri Smail	✓		✓	✓			✓			✓	✓		✓	✓
Benhammou Aissa	✓	✓	✓	✓	✓	✓		✓	✓	✓			✓	

C : **C**onceptualization
M : **M**ethodology
So : **So**ftware
Va : **Va**lidation
Fo : **Fo**rmal analysis
I : **I**nvestigation
R : **R**esources
D : **D**ata Curation
O : Writing - **O**riginal Draft
E : Writing - Review & **E**diting
Vi : **Vi**sualization
Su : **Su**pervision
P : **P**roject administration
Fu : **Fu**nding acquisition

CONFLICT OF INTEREST STATEMENT

The authors declare that they have no conflicts of interest.

DATA AVAILABILITY

The data supporting the results of this study are available from the corresponding author, TN, upon reasonable request.

REFERENCES

[1] A. Albatayneh, M. N. Assaf, D. Alterman, and M. Jaradat, "Comparison of the overall energy efficiency for internal combustion engine vehicles and electric vehicles," *Environmental and Climate Technologies*, vol. 24, no. 1, pp. 669–680, Jan. 2020, doi: 10.2478/rtuect-2020-0041.

[2] Z. Liu *et al.*, "Carbon monitor, a near-real-time daily dataset of global CO2 emission from fossil fuel and cement production," *Scientific Data*, vol. 7, no. 1, p. 392, Nov. 2020, doi: 10.1038/s41597-020-00708-7.

[3] John D. Graham, *The global rise of the modern plug-in electric vehicle*. Edward Elgar Publishing, 2021.

[4] J. Cao, X. Chen, R. Qiu, and S. Hou, "Electric vehicle industry sustainable development with a stakeholder engagement system," *Technology in Society*, vol. 67, p. 101771, Nov. 2021, doi: 10.1016/j.techsoc.2021.101771.

[5] C. Sain, A. Banerjee, and P. K. Biswas, *Control strategies of permanent magnet synchronous motor drive for electric vehicles*. CRC Press, 2022.

[6] M. Monadi, M. Nabipour, F. Akbari-Behbahani, and E. Pouresmaeil, "Speed control techniques for permanent magnet synchronous motors in electric vehicle applications toward sustainable energy mobility: a review," *IEEE Access*, vol. 12, pp. 119615–119632, 2024, doi: 10.1109/ACCESS.2024.3450199.

[7] H. Farzin and M. Monadi, "Reliability enhancement of active distribution grids via emergency V2G programs: An analytical cost/worth evaluation framework," *Scientia Iranica*, vol. 26, no. 6, pp. 3635–3645, Sep. 2019, doi: 10.24200/sci.2019.54158.3624.

[8] W. Lang, Y. Hu, C. Gong, X. Zhang, H. Xu, and J. Deng, "Artificial intelligence-based technique for fault detection and diagnosis of EV motors: a review," *IEEE Transactions on Transportation Electrification*, vol. 8, no. 1, pp. 384–406, Mar. 2022, doi: 10.1109/TTE.2021.3110318.

[9] D. Rimpas, S. D. Kaminaris, D. D. Piromalis, G. Vokas, K. G. Arvanitis, and C. S. Karavas, "Comparative review of motor technologies for electric vehicles powered by a hybrid energy storage system based on multi-criteria analysis," *Energies*, vol. 16, no. 6, p. 2555, Mar. 2023, doi: 10.3390/en16062555.

[10] V. J. Bobin and M. M. Beno, "Performance analysis of optimization based FOC and DTC methods for three phase induction motor," *Intelligent Automation and Soft Computing*, vol. 35, no. 2, pp. 2493–2511, 2023, doi: 10.32604/iasc.2023.024679.

[11] B. K. Bose, "Power electronics-a technology review," *Proceedings of the IEEE*, vol. 80, no. 8, pp. 1303–1334, 1992, doi: 10.1109/5.158603.

[12] H. Mesloub, R. Boumaaraf, M. T. Benchouia, A. Goléa, N. Goléa, and K. Srairi, "Comparative study of conventional DTC and

DTC_SVM based control of PMSM motor — Simulation and experimental results," *Mathematics and Computers in Simulation*, vol. 167, pp. 296–307, Jan. 2020, doi: 10.1016/j.matcom.2018.06.003.
[13] J. Agarwal, G. Parmar, R. Gupta, and A. Sikander, "Analysis of grey wolf optimizer based fractional order PID controller in speed control of DC motor," *Microsystem Technologies*, vol. 24, no. 12, pp. 4997–5006, Apr. 2018, doi: 10.1007/s00542-018-3920-4.
[14] Y. Ahmed, A. Hoballah, E. Hendawi, S. Al Otaibi, S. K. Elsayed, and N. I. Elkalashy, "Fractional order PID controller adaptation for pmsm drive using hybrid grey wolf optimization," *International Journal of Power Electronics and Drive Systems*, vol. 12, no. 2, pp. 745–756, Jun. 2021, doi: 10.11591/ijpeds.v12.i2.pp745-756.
[15] K. Hartani, Y. Miloud, and A. Miloudi, "Electric vehicle stability with rear electronic differential traction," *EFEEA'10 International Symposium on Environment Friendly Energies in Electrical Applications*, pp. 1–5, 2010.
[16] H. Ben Achour, S. Ziani, Y. Chaou, Y. El Hassouani, and A. Daoudia, "Permanent magnet synchronous motor PMSM control by combining vector and PI controller," *WSEAS Transactions on Systems and Control*, vol. 17, pp. 244–249, May 2022, doi: 10.37394/23203.2022.17.28.
[17] L. Shi, M. Lv, and P. Li, "Sensorless position control in high-speed domain of PMSM based on improved adaptive sliding mode observer," *Processes*, vol. 12, no. 11, p. 2581, Nov. 2024, doi: 10.3390/pr12112581.
[18] D. Il Son, J. S. Han, J. S. Park, H. S. Lim, and G. H. Lee, "Performance improvement of DTC-SVM of PMSM with compensation for the dead time effect and power switch loss based on extended Kalman filter," *Electronics (Switzerland)*, vol. 12, no. 4, p. 966, Feb. 2023, doi: 10.3390/electronics12040966.
[19] S. Sondhi and Y. V Hote, "Fractional order controller and its applications: A review," in *Proceedings of the 2nd IASTED Asian Conference on Modelling, Identification, and Control, AsiaMIC 2012*, 2012, pp. 118–123, doi: 10.2316/P.2012.769-089.
[20] S. Sondhi and Y. V Hote, "Fractional order PID controller for load frequency control," *Energy Conversion and Management*, vol. 85, pp. 343–353, Sep. 2014, doi: 10.1016/j.enconman.2014.05.091.
[21] X. Ding, R. Li, Y. Cheng, Q. Liu, and J. Liu, "Design of and research into a multiple-fuzzy pid suspension control system based on road recognition," *Processes*, vol. 9, no. 12, p. 2190, Dec. 2021, doi: 10.3390/pr9122190.
[22] I. Podlubny, "Fractional-order systems and PIλDμ-controllers," *IEEE Transactions on Automatic Control*, vol. 44, no. 1, pp. 208–214, Jan. 1999, doi: 10.1109/9.739144.
[23] M. Y. Silaa, O. Barambones, M. Derbeli, C. Napole, and A. Bencherif, "Fractional order PID design for a proton exchange membrane fuel cell system using an extended grey wolf optimizer," *Processes*, vol. 10, no. 3, p. 450, Feb. 2022, doi: 10.3390/pr10030450.
[24] S. Mirjalili, S. M. Mirjalili, and A. Lewis, "Grey wolf optimizer," *Advances in Engineering Software*, vol. 69, pp. 46–61, Mar. 2014, doi: 10.1016/j.advengsoft.2013.12.007.
[25] Y. Hou, H. Gao, Z. Wang, and C. Du, "Improved grey wolf optimization algorithm and application," *Sensors*, vol. 22, no. 10, p. 3810, May 2022, doi: 10.3390/s22103810.
[26] M. K. Kar, S. Kumar, A. K. Singh, S. Panigrahi, and M. Cherukuri, "Design and analysis of FOPID-based damping controllers using a modified grey wolf optimization algorithm," *International Transactions on Electrical Energy Systems*, vol. 2022, pp. 1–31, Oct. 2022, doi: 10.1155/2022/5339630.
[27] T. Nawal, O.-A. Omar, M. Smail, and B. Aissa, "Enhanced dynamics of sensorless two-wheel drive electric vehicles through electronic differential and advanced metaheuristic algorithms," *Studies in Engineering and Exact Sciences*, vol. 5, no. 2, p. e11890, Dec. 2024, doi: 10.54021/seesv5n2-718.
[28] O. Khaddam, "Electric vehicle technology," in *Active Electrical Distribution Network: Issues, Solution Techniques, and Applications*, Elsevier, 2022, pp. 97–119.
[29] A. Ravi and S. Palani, "Robust electronic differential controller for an electric vehicle," *American Journal of Applied Sciences*, vol. 10, no. 11, pp. 1356–1362, Nov. 2013, doi: 10.3844/ajassp.2013.1356.1362.

BIOGRAPHIES OF AUTHORS

Touhami Nawal is a Ph.D. student in electrical engineering at Ahmed Draia University of Adrar, Algeria. She obtained a master's diploma in electrical engineering, specializing in electric control, from Tahri Mohammed University of Bechar in Algeria in 2018. Her research interests focus on the field of electrical engineering, such as electric vehicle control, energy management, and optimization algorithms. She can be contacted at email: touhami.nawal@univ-adrar.edu.dz.

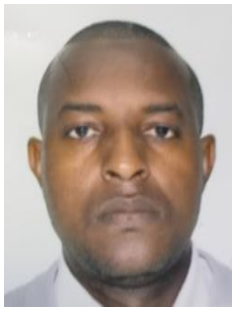

Ouled-Ali Omar is a lecturer and a member of the LDDI Laboratory at Ahmed Draia University in Adrar. He earned his Ph.D. in electrical engineering from the Faculty of Electrical Engineering at Djillali Liabes University, Sidi Bel Abbes, in 2021. His research interests include robust, advanced, and intelligent control methods for AC drives, power electronic converters, renewable energy, and electric vehicles. He can be reached via email: ouleomar@univ-adrar.edu.dz.

Mansouri Smail received a bachelor's degree in electronics education from the School of Secondary Teachers in Oran, Algeria, in 1993, and a master's degree in automatic from Bechar University, Bechar, Algeria, in 2013. In 2017, he completed a Ph.D. degree in electronics engineering at Bechar University, Bechar, Algeria. Between 1993 and 2013, he worked as a secondary school teacher. Currently, he is an associate professor in the Department of Fuels and Renewables Energy, Faculty of Engineering at the University of Adrar, Algeria. Dr. Mansouri can be contacted at email: mansouri197105@univ-adrar.edu.dz.

Benhammou Aissa is a doctor in industrial electrotechnical. He obtained his master's degree from Tahri Mohamed University of Bechar in 2019 and his Ph.D. from Nour Elbachir University Center of El-Bayadh in 2023. His research interests encompass electric vehicles, drone systems, power electronics, optimization algorithms, and electrostatics separation. Dr. Benhammou can be contacted via email at benhammou.aissa@univ-bechar.dz.